DOI 10.5162/Ultrasonic2025/A18-a3

Identification of temperature-dependent material parameter functions in piezoelectricity

Raphael Kuess[1], Olga Friesen[2], Bernd Henning[2], and Andrea Walther[1]
[1] Humboldt-Universität zu Berlin, Unter den Linden 6, 10099 Berlin, Germany
[2] Paderborn University, Warburger Straße 100, 33098 Paderborn, Germany
raphael.kuess@hu-berlin.de

Abstract: We address the problem of identifying the temperature-dependent parameters of ring-shaped piezoelectric samples based on simulated data. For this purpose, we assume a polynomial structure of the material parameters with respect to the temperature. To increase stability and accuracy of the reconstruction, we apply adapted optimization and regularization strategies using regularized Newton-type methods in a block coordinate descent framework.

Keywords: Inverse Problems, Piezoelectricity, Temperature dependence, Parameter identification, Regularization

Introduction

Understanding the behavior of piezoelectric components is essential for various sensor and actuator applications, especially given their temperature-dependent characteristics. While piezoceramic elements undergo changes in properties due to heating during operation, it is imperative to develop a method for predicting these changes. This results in the assumption that the material parameters depend on temperature changes, where we do not consider thermal coupling effects. The elastic stiffness parameter c^{E} is not very sensitive to temperature changes, see [1]. Hence, we assume that this parameter is known, yielding that the required matrix valued parameter functions for the piezoelectric coupling e and the permittivity ε^{S} are dependent on a known temperature $\theta \in \Theta$:

$$e(\theta) := \begin{pmatrix} 0 & 0 & 0 & e_{15}(\theta) \\ e_{31}(\theta) & e_{31}(\theta) & e_{33}(\theta) & 0 \end{pmatrix}, \quad (1)$$

$$\varepsilon^{\mathrm{S}}(\theta) := \begin{pmatrix} \varepsilon_{11}(\theta) & 0 \\ 0 & \varepsilon_{33}(\theta) \end{pmatrix}, \quad (2)$$

where $\Theta \subset \mathbb{R}^+$ is a temperature interval of finite cardinality. Furthermore, we deduce from [1] that it is reasonable to assume a polynomial structure of the material parameters with respect to θ, i.e.,

$$(e(\theta), \varepsilon(\theta)) = \left(\sum_{j=0}^{k} a_j \theta^j, \sum_{j=0}^{k} b_j \theta^j \right), \quad (3)$$

where $(a_j, b_j) \in \mathbb{R}^{2\times 4} \times \mathbb{R}^{2\times 2}$ for $0 \leq j \leq k$. The coefficients in (3) are constant matrices and have the same structure as in the identities (1)-(2). This results in a transition of the parameter function space to a finite dimensional vector space, see [2].

The inverse problem

For $k = 1$, we have to reconstruct 10 parameters. Consequently, the parameter space X reads as

$$X := \Big\{ p \in \mathbb{R}^{10} : \; p_1 = a_{11_0} > 0, \; p_2 = a_{33_0} > 0, \; p_3 = b_{15_0}, \; p_4 = b_{31_0}, \; p_5 = b_{33_0}, \; p_6 = a_{11_1}, \; p_7 = a_{33_1}, \; p_8 = b_{15_1}, \; p_9 = b_{31_1}, \; p_{10} = b_{33_1} \Big\}.$$

As geometry we consider a thin annular piezoelectric element, where we exploit the symmetry of the geometry and use cylindrical instead of Cartesian coordinates. Consequently, we obtain a Lipschitz domain $\Omega \subset \mathbb{R}^2$ and assume that its boundary can be represented as the disjoint union $\partial\Omega := \Gamma_a \dot\cup \Gamma_0 \dot\cup \Gamma_n$. Thereby, Γ_a is the boundary segment electrically excited with an excitation signal independent of the spatial domain (equally distributed), Γ_0 is the grounded boundary segment and Γ_n is the remaining part of $\partial\Omega$. We introduce

$$H^2_{0,\Gamma}(\Omega, \mathbb{C}) = \left\{ f \in H^2(\Omega, \mathbb{C}) |\; f|_{(\Gamma_a \cup \Gamma_0)} = 0 \right\},$$

$$H^2_{\mathcal{B}}(\Omega, \mathbb{C}^2) = \Big\{ f \in L^2(\Omega, \mathbb{C}^2) |\; \|f\|_{H^2_{\mathcal{B}}(\Omega,\mathbb{C}^2)} := \|f\|_{L^2(\Omega,\mathbb{C}^2)} + \|\mathcal{B}f\|_{L^2(\Omega,\mathbb{C}^2)} + \left\|\mathcal{B}^T\mathcal{B}f\right\|_{L^2(\Omega,\mathbb{C}^2)} \Big\},$$

where

$$\nabla := \begin{pmatrix} \frac{\partial}{\partial r} \\ \frac{\partial}{\partial z} \end{pmatrix} \text{ and } \mathcal{B} := \begin{pmatrix} \frac{\partial}{\partial r} & 0 \\ \frac{1}{r} & 0 \\ 0 & \frac{\partial}{\partial z} \\ \frac{\partial}{\partial z} & \frac{\partial}{\partial r} \end{pmatrix},$$

with r denoting the radial and z the spatial element. Hence, we define the state space as

$$W := \left(H^2_{\mathcal{B}}(\Omega, \mathbb{C}^2) \times H^2_{0,\Gamma}(\Omega, \mathbb{C}) \right),$$

which coincides with the solution space of the following Fourier-transformed PDE-system

$$\begin{aligned}
&\forall\theta\in\Theta,\ \forall\omega\in\mathcal{W}:\\
&-\rho\omega^2 d_1\hat{u}-\mathcal{B}^{\mathrm{T}}\big(d_2 c^{\mathrm{E}}(\theta)\mathcal{B}\hat{u}+e^{\mathrm{T}}(\theta)\nabla\hat{\phi}_0\big)\\
&\qquad=\mathcal{B}^{\mathrm{T}}e^{\mathrm{T}}(\theta)\nabla\chi \quad \text{in } \Omega \quad (4)\\
&-\nabla\cdot\Big(e(\theta)\mathcal{B}\hat{u}-\varepsilon^{\mathrm{S}}(\theta)\nabla\hat{\phi}_0\Big)\\
&\qquad=-\nabla\cdot\varepsilon^{\mathrm{S}}(\theta)\nabla\chi \text{ in } \Omega \quad (5)\\
&n\cdot\Big(e(\theta)\mathcal{B}\hat{u}-\varepsilon^{\mathrm{S}}(\theta)\nabla\hat{\phi}_0\Big)\\
&\qquad=n\cdot\varepsilon^{\mathrm{S}}(\theta)\nabla\chi \quad \text{on } \Gamma_{\mathrm{n}} \quad (6)\\
&\mathcal{N}^{\mathrm{T}}\big(d_2 c^{\mathrm{E}}(\theta)\mathcal{B}\hat{u}+e^{\mathrm{T}}(\theta)\nabla\hat{\phi}_0\big)\\
&\qquad=-\mathcal{N}^{\mathrm{T}}e^{\mathrm{T}}(\theta)\nabla\chi \text{ on } \partial\Omega, \quad (7)
\end{aligned}$$

where $s=(\hat{u},\hat{\phi}_0)$ is the solution of the system, $\rho\in\mathbb{R}^+$, $d_1:=1-\mathrm{i}\frac{\alpha}{\omega}$, $d_2:=1+\mathrm{i}\omega\beta$. We denote the space of frequencies with $\mathcal{W}\subset\mathbb{R}^+$, $|\mathcal{W}|<\infty$. Furthermore, n is the normal element corresponding to ∇ and $\mathcal{N}$ the normal element corresponding to $\mathcal{B}$. Additionally, we included the Rayleigh damping model, with $\alpha,\beta\in\mathbb{R}_0^+$ as Rayleigh damping parameters. The mixed Dirichlet boundary conditions, needed to model the excitation behavior, were homogenized using the Dirichlet lift Ansatz with Dirichlet lift function χ, see [2]. Consequently, we define the piezoelectric model operator $A_\omega^\theta: X\times W\to W^*$ for each $\theta\in\Theta$ and $\omega\in\mathcal{W}$ via

$$\begin{aligned}
&\langle A_\omega^\theta(p,s),(v,w)\rangle_{W^*,W}:=2\pi\int_\Omega\Big(-d_1\rho\omega^2\hat{u}^{\mathrm{T}}\overline{v}\\
&+\Big(d_2 c^{\mathrm{E}}(\theta)\mathcal{B}\hat{u}+e^{\mathrm{T}}(\theta)\nabla\hat{\phi}_0\Big)^{\mathrm{T}}\overline{\mathcal{B}v}\\
&+\Big(e(\theta)\mathcal{B}\hat{u}-\varepsilon^{\mathrm{S}}(\theta)\nabla\hat{\phi}_0\Big)^{\mathrm{T}}\overline{\nabla w} \quad (8)\\
&+(e^{\mathrm{T}}(\theta)\nabla\chi)^{\mathrm{T}}\overline{\mathcal{B}v}-(\varepsilon^{\mathrm{S}}(\theta)\nabla\chi)^{\mathrm{T}}\overline{\nabla w}\Big)r\,\mathrm{d}(r,z)\,.
\end{aligned}$$

To recover information on the parameter p, we need observed data with respect to the state s and the parameters p. Hence, we define the charge pulse $Q_\omega^\theta:\ X\times W\to\mathbb{C}$,

$$\begin{aligned}
&Q_\omega^\theta(p,s)=\mathrm{Re}\left(Q_\omega^\theta(p,s)\right)+\mathrm{Im}\left(Q_\omega^\theta(p,s)\right)\\
&=2\pi\int_{\Gamma_a}r\left(e(\theta)\mathcal{B}\hat{u}-\varepsilon^{\mathrm{S}}(\theta)\nabla\hat{\phi}\right)\cdot n\,\mathrm{d}(r,z) \quad (9)
\end{aligned}$$

for each $\theta\in\Theta,\ \omega\in\mathcal{W}$, where $\mathrm{Re}(\cdot)$ denotes the real and $\mathrm{Im}(\cdot)$ the imaginary parts. We assume that $\left\|Q_\omega^\theta\right\|_{\mathbb{C}}>0$ and define the observation operator $C_\omega^\theta:\ X\times W\to\mathbb{R}$ for each $\theta\in\Theta,\ \omega\in\mathcal{W}$ as

$$C_\omega^\theta(p,z)=\log\left(\left\|Q_\omega^\theta\right\|_{\mathbb{C}}\right). \quad (10)$$

To model the inverse problem, we employ the reduced approach, meaning that we have to eliminate the model by introducing a so-called parameter-to-state map S_ω^θ for each $\omega\in\mathcal{W}$ and each $\theta\in\Theta$, which maps each parameter to the corresponding solution of the underlying PDE model (4)-(7). For existence and regularity of the parameter-to-state we need the following result, which includes regularities and important properties of the model and the observation operator.

Proposition 1. *For each $\omega\in\mathcal{W}$ and $\theta\in\Theta$, A_ω^θ as given in* (8) *is well-defined, bounded, bijective and continuously Fréchet differentiable on $X\times W$, C_ω^θ as given in (10) is well-defined, bounded and continuously Fréchet differentiable on $X\times W$ and S_ω^θ is well-defined, non-linear and continuously Fréchet differentiable on X.*

Proof. Due to Plancherel's Theorem, see [3], Chapter 7, the Fourier transform is continuously invertible on $L^2(0,T)$. Furthermore, the coordinate transformation is continuously invertible and $H^1(0,T)$ is isometrically isomorphic to $L^2(0,T)$. Hence, there exists a continuously invertible transformation between our setting and the setting in [2]. Lastly, $\left\|Q_\omega^\theta\right\|_{\mathbb{C}}>0$, $\|\cdot\|$ on $\mathbb{R}\setminus\{0\}$ and $\log(\cdot)$ on $\mathbb{R}^+$ are continuously Fréchet differentiable. □

As observed data is usually contaminated with noise, we consider noisy data $y^\delta\in\mathbb{R}^{|\mathcal{W}|\cdot|\Theta|}$. Then, the forward operator $F:X\to\mathbb{R}^{|\mathcal{W}|\cdot|\Theta|}$ reads as

$$F(p)=\begin{pmatrix}\left(C_\omega^{\theta_1}(p,S_\omega^{\theta_1}(p))\right)_{\omega\in\mathcal{W}}\\ \vdots\\ \left(C_\omega^{\theta_{|\Theta|}}(p,S_\omega^{\theta_{|\Theta|}}(p))\right)_{\omega\in\mathcal{W}}\end{pmatrix}.$$

Consequently, we want to identify $p\in X$ such that

$$F(p)=y^\delta. \quad (11)$$

This casts the problem into a single operator equation for the quantity p. As this inverse problem is ill-posed, see [4], we introduce a weakly lower semi-continuous regularizer $\mathcal{R}_\tau:X\to\mathbb{R}$ with regularization parameter $\tau>0$. Then, we address the inverse problem (11) similarly to [2] and [4] via an optimization approach, i.e., we aim at finding a minimizer of

$$J(p):=\frac{1}{2}\left\|F(p)-y^\delta\right\|^2_{\mathbb{R}^{|\mathcal{W}||\Theta|}}+\mathcal{R}_\tau(p), \quad (12)$$

which we assume to exist. As gradient computation for J in (12) is often done via adjoints, we note that the adjoint PDE is uniquely solvable for every state $(\hat{u},\hat{\phi}_0)\in W$, see Proposition 1 and [2].

Numerical realization and results

In praxis, sensitivities for different parameters vary considerably for solution methods to inverse problems in piezoelectricity, see [5]. To provide a better

handling of sensitivities, we propose a block coordinate descent (BCD) approach, similarly to [5]. This method iteratively minimizes the objective function over selected blocks of optimization variables while keeping the remaining optimization variables fixed, see [6]. We assume a cyclic selection, which means that the same partitions in a fixed order are cycled through, where in each step, one block is updated according to a sub-optimization method and then fixed while the next block is optimized. As [5] suggests to use BCD methods in combination with Newton-type methods as sub-optimization method, we apply a regularized structure exploiting Quasi-Newton update, see [7]. To ensure robustness we use the globalized approach (GRSE) of [7], which controls the regularization parameter such that it leads to globalization. Furthermore, we will use the partition $B_1 := \{a_{33_l}, b_{15_l}, b_{31_l}, b_{33_l} : l = 1, 2\}$ and $B_2 := \{a_{11_l} : l = 1, 2\}$. This choice is motivated by the corresponding sensitivities, since the forward operator is least sensitive to a_{11_0} for zeroth-order parameters and to a_{11_1} for first-order parameters. Consequently, it is reasonable to perform the optimization for B_1 first, while keeping B_2 fixed at the initial guess until convergence is reached to some extent, and then start with the alternating reconstruction of both blocks. As each block performs the GRSE method, they may have own regularization parameters $\tau^{B_1} > 0,\ \tau^{B_2} > 0$ corresponding to the respective block. The inverse problem will be numerically realized using the discretize-then-optimize approach, where we employ algorithmic differentiation (AD), see [8] and [9]. The space discretization is based on a finite element method, where we use FEniCS [10] in dolfin version 2019.2.0.dev0 and AD via the dolfin adjoint [11] library of FEniCS in version 2019.1.0. As domain Ω we consider a rectangle with vertices $(2.6, 0),\ (6.35, 0),\ (6.35, 1),\ (2.6, 1)$, where coordinates are given in mm. Furthermore, we use $10\,\mathrm{V}$ as excitation pulse and perform any numerical realization in kHz. This has the advantage of a better condition of the PDE system as the magnitudes of the material parameters differ significantly less. The temperature values considered in all numerical realizations will be $\Theta = \{50\,^\circ\mathrm{C},\ 70\,^\circ\mathrm{C}\}$. The damping parameters and the elastic stiffness parameter at $60\,^\circ\mathrm{C}$ are taken from [1]. The polynomial parameters serving as ground truth p^* are presented in Tab. 1 according to [1], rounded to two decimal places. Using FEniCS, specifying the Dirichlet lift function χ can be avoided, as it is possible to directly implement mixed Dirichlet conditions. Third-order elements with element size $h = 150\,\mu\mathrm{m}$ yield sufficiently reasonable simulation outcomes. From

Tab. 1: Target polynomial parameters.

Pol. par.	Value	Pol. par.	Value
a_{11_0}	2505.38	b_{15_1}	11.34
a_{11_1}	9.72	b_{31_0}	-5045.55
a_{33_0}	4975.13	b_{31_1}	-7.35
a_{33_1}	18.67	b_{33_0}	13 316.54
b_{15_0}	9174.08	b_{33_1}	23.82

[12] and computed sensitivities, conclusions can be drawn about reasonable frequency domains for the inverse problem. Due to the small sensitivities of the forward operator with respect to a_{11_0} and a_{11_1}, we will use a finer frequency grid in areas where the forward operator is more sensitive to those parameters and in resonance areas. Hence, we use $\mathcal{W} := \mathcal{W}_1 \cup \mathcal{W}_2 \cup \mathcal{W}_3$ as frequency domain, where

$$\mathcal{W}_1 := \{\omega \in \mathbb{N} :\ \omega \equiv 0 \bmod 3,\ 38 \leq \omega < 2600\},$$
$$\mathcal{W}_2 := \{\omega \in \mathbb{N} :\ \omega \equiv 0 \bmod 20,\ 2600 \leq \omega < 4500\},$$
$$\mathcal{W}_3 := \{\omega \in \mathbb{N} :\ \omega \equiv 0 \bmod 3,\ 4500 \leq \omega \leq 6000\}.$$

To generate the noisy data y^δ we contaminate the exact simulated data y, generated according to the parameters in Tab. 1, additively with uniformly distributed random noise with a noise level of 1%. We employ the hyperparameters $\mu = 0.5$, $\tau_0^{B_1} = \tau_0^{B_2} = 10^{-1}$, $\sigma = 4$, $c = a = 10^{-2}$ and scale the zeroth-order parameters with 10^2. Here, μ is the decay factor and σ is the growth factor of the regularization parameters for each block, see [7], and $c,\ a$ refer to $c,\ p$ in [7]. As initial Quasi-Newton matrices for each block we use scaled identities with scaling factor 10^{-4}. Finally, we choose an initial parameter guess p^0 that deviates by 5% from the parameters in Tab. 1. In Fig. 1, the parameter identification results using the BCD-GRSE method are shown, where every iteration step remained in the feasible set. For better visualization, the reconstructed parameter values have been normed by the ground truth, such that we aim for convergence to one. The reconstruction results in Fig. 1 show convergence, but the parameters to which the forward operator is least sensitive overall do not fully align with the respective ground truth. However, the charge computed with the reconstructed parameters aligns very well with the one obtained with the target parameters. The convergence of the data discrepancy term of the objective function to the target value confirms this behavior, see Fig. 2, where p^n denotes the reconstructed parameter at iteration n. Consequently, no further improvements can be expected, given the current objective function, since the occurrence of various

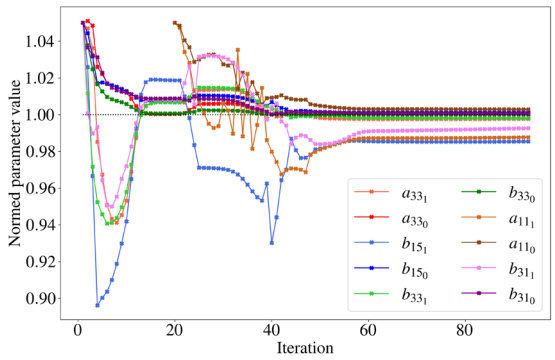

Fig. 1: Identification of the polynomial parameters.

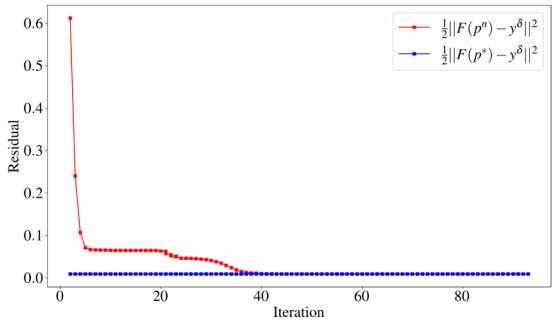

Fig. 2: Convergence of the data discrepancy.

local minima impairs uniqueness of reconstructed parameters. This behavior appears to occur due to the amplification of the discrepancy in sensitivities by the forward operator in the parameterized case. Consequently, selecting a suitable frequency range led to an improvement. If the material parameters are reconstructed separately for each individual temperature, this effect occurs significantly less.

Conclusion

We considered the problem of identifying temperature-dependent material parameters for piezoelectric rings, where we assumed a polynomial structure of the material parameters with respect to the temperature. To achieve reliable parameter identification, we used a block coordinate descent regularized Quasi-Newton method and adapted the frequency domain. The resulting methodology allowed a sufficient reconstruction of the polynomial parameters, as demonstrated by numerical results, but is prone to instability with respect to uniqueness. Furthermore, we note that this approach relies on a-priori knowledge of the parameter behavior, which is reasonable but may not always be available.

Acknowledgements

The authors thank the German Research Foundation (DFG) for financial support within the research group 5208 NEPTUN (444955436), support code JU 3254/1-1 and WA 1607/21-1. The work on this paper was partly funded by the DFG under Germany´s Excellence Strategy – The Berlin Mathematics Research Center MATH+ (EXC-2046/1, project ID: 390685689).

References

[1] O. Friesen et al. “Estimation of temperature-dependent piezoelectric material parameters using ring-shaped specimens”. In: *Journal of Physics: Conference Series* 2822.1 (2024), p. 012125.

[2] R. Kuess, D. Walter, and A. Walther. *Modelling and Analysis of an Inverse Parameter Identification Problem in Piezoelectricity*. Tech. rep. 2025.

[3] J. Cerdà. *Linear functional analysis*. Vol. 116. American Mathematical Soc., 2010.

[4] T. Lahmer. “Forward and Inverse Problems in Piezoelectricity”. doctoral thesis. Friedrich-Alexander-Universität Erlangen-Nürnberg, 2008.

[5] B. Jurgelucks. “Increased Sensitivity in Parameter Identification Problems for Piezoelectrics”. doctoral thesis. Paderborn University, 2019.

[6] S. Wright. “Coordinate descent algorithms”. In: *Math. Programming* 151.1 (2015), pp. 3–34.

[7] R. Kuess and A. Walther. *On regularized structure exploiting Quasi-Newton methods for ill-posed problems*. Tech. rep. 2025.

[8] R. Griesse and A. Walther. “Evaluating gradients in optimal control: continuous adjoints versus automatic differentiation”. In: *J. of Opt. Theory and App.* 122 (2004), pp. 63–86.

[9] A. Griewank and A. Walther. *Evaluating Derivatives*. Second edition. Society for Industrial and Applied Mathematics, 2008.

[10] M. Alnæs et al. “The FEniCS project version 1.5”. In: *Archive of Numerical Software* 3 (2015).

[11] S. Mitusch, S. Funke, and J. Dokken. “dolfin-adjoint 2018.1: automated adjoints for FEniCS and Firedrake”. In: *Journal of Open Source Software* 4.38 (2019), p. 1292.

[12] O. Friesen et al. “Estimation of piezoelectric material parameters of ring-shaped specimens”. In: *tm - Technisches Messen* (2024).